Discrimination methodologies using femtosecond LIBS and correlation techniques

Sunku Sreedhar, E. Nageswara Rao, G. Manoj Kumar,[a] Surya P. Tewari, S. Venugopal Rao[*]

*Advanced Centre of Research in High Energy Materials **(ACRHEM),***
University of Hyderabad, Prof. C. R. Rao Road,
Gachibowli, Hyderabad 500046, India
, [a] Authors for correspondence: **svrsp@uohyd.ernet.in; **manojsp@uohyd.ernet.in***

Abstract

Laser induced breakdown spectroscopy is an attractive and versatile spectroscopic technique employed successfully for the detection of hazardous substances. The specific advantages of using femtosecond (fs) pulses with LIBS technique include lower ablation threshold, reduced background Continuum emission. In addition to atomic peaks in plasma the molecular peaks (CN and C_2) also play a significant role in classification of these samples. In the present work fs LIBS spectra were recorded from five different samples (RDX, HMX, NTO, ANTA, and DADNE) made in the form of pure pellets. Correlation statistics were used to discriminate the samples based on molecular, atomic ratios. This paper discusses, in detail, a simple correlation technique applied for the fs LIBS data for achieving classification.

Introduction

Laser induced breakdown spectroscopy (LIBS) has been acknowledged as an attractive and a versatile spectroscopic technique for the detection of hazardous substances [1] such as explosives with encouraging attributes such as stand-off detection capability, prospective trace material discovery, and high speed detection [3-8]. LIBS technique typically employs a pulsed laser (nanosecond/ femtosecond) to produce breakdown on the surface of sample to be examined. The hot dense plasma is formed after the breakdown. The created hot plasma in the process of cooling emits radiation. The emitted light is collected with a spectrometer and the collected spectra consist of several sharp peaks, characteristic of elemental species present in the sample [9-11]. Femtosecond (fs) laser as an excitation source has recently been added to LIBS techniques to create plasma and perform spectroscopic studies. Fs laser plasma can be created with lower incident laser energy and ablation threshold compared to the nanosecond (ns) case. Furthermore, the produced plasma emits a nearly background less Continuum [12]. In comparison to ns LIBS, fs laser produced plasma has negligible interaction with the input pulses. Furthermore, the possibility of performing remote detection with filament induced breakdown using ultrashort lasers makes it even more practical [13]. Gordon and his co workers demonstrated that using polarization resolving technique good S/N ratios fs LIBS spectra were recorded with non-gated spectrometer [14-15]. Baudelet et al. demonstrated the detection of bacterial trace samples effectively using fs LIBS [16-17]. Detection of several explosives has been made possible with fs lasers by several groups in trace form [18-20] and in pure form [21-22].

Most of the energetic materials are composed of hydrogen, carbon, oxygen, and nitrogen exhibiting similar molecular and elemental signatures in their LIBS spectra. The task of identifying one material from the other is not straight forward. In addition to atomic peaks, the molecular peaks (such as CN and C_2) play an important role in classifying these samples. Careful analysis is required to identify an exact HEM. Several statistical techniques have been utilized by many groups to classify several explosive samples using molecular and atomic peaks [24-27]. Utilization of different statistical techniques need some treatment of some preprocessing is necessary. In this work we demonstrated the technique using elemental/molecular ratios with different 2D ratios combination. The present study exploring effort has been made to discriminate HEMs to classify the several chemical warfare samples like RDX ($C_3H_6N_6O_6$), HMX ($C_4H_8N_8O_8$), NTO ($C_2H_2N_4O_3$), ANTA ($C_2H_3N_5O_2$) and DADNE ($C_2H_4N_4O_4$). All the compounds were having the similar elemental composition.

Next-Generation Spectroscopic Technologies VI, edited by Mark A. Druy, Richard A. Crocombe, Proc. of SPIE Vol. 8726, 87260H · © 2013 SPIE
CCC code: 0277-786X/13/$18 · doi: 10.1117/12.2015749

Experimental Setup

Amplified Ti:sapphire laser pulses with duration of ~40 fs, maximum energy of 2.5 mJ delivered at a repetition rate of 1 kHz (central wavelength of 800 nm) were used in all the experiments. The samples were made in the form of a pellet by first grinding the sample with agate mortar and then applying 10 ton hydraulic pressure onto the powdered sample. The fs laser pulses were focused on the target sample mounted on XY translation stage with 8 cm plano-convex lens. The energy used to produce plasma was ~1.2 mJ and corresponding fluence estimated was ~22 J/cm^2. A collection lens system unit was placed to collect the light from plasma and light passed through a fiber optic cable and finally transferred to a gated ICCD spectrometer (Andor i-star DH734 ICCD + ME 5000 Mechelle spectrograph, resolution 5000). Argon gas was purged through a nozzle onto the sample where laser pulses were focused on to the pellets.

Results and discussion:

Figure 1 shows the LIBS spectra of different explosives recorded with fs laser pulses in argon atmosphere. A gate delay 100 ns and gate width 800 ns were used for recording the spectra. The elemental peaks corresponding to C-247.82 nm, N-821.50 nm, 822.35 nm, 867.80 nm, 868.80 nm, O-777.2, 844.55 nm and H-656.2 nm lines and molecular peaks of CN in between 385-389 nm range were observed in the spectra. These spectral features play a significant role in discrimination of these samples. In LIBS technique, the ablated volumetric mass directly represents the composition of sample constituents, this will reflect in the LIBS spectrum. All 5 samples have same elements C, H, N and O with different composition. So the spectral emission from LIBS plasma offered similar peaks with different magnitudes as shown in the figure 1. The classification of these samples using obtained LIBS spectra is a difficult task. Therefore, precise statistical techniques are needed to classify these samples.

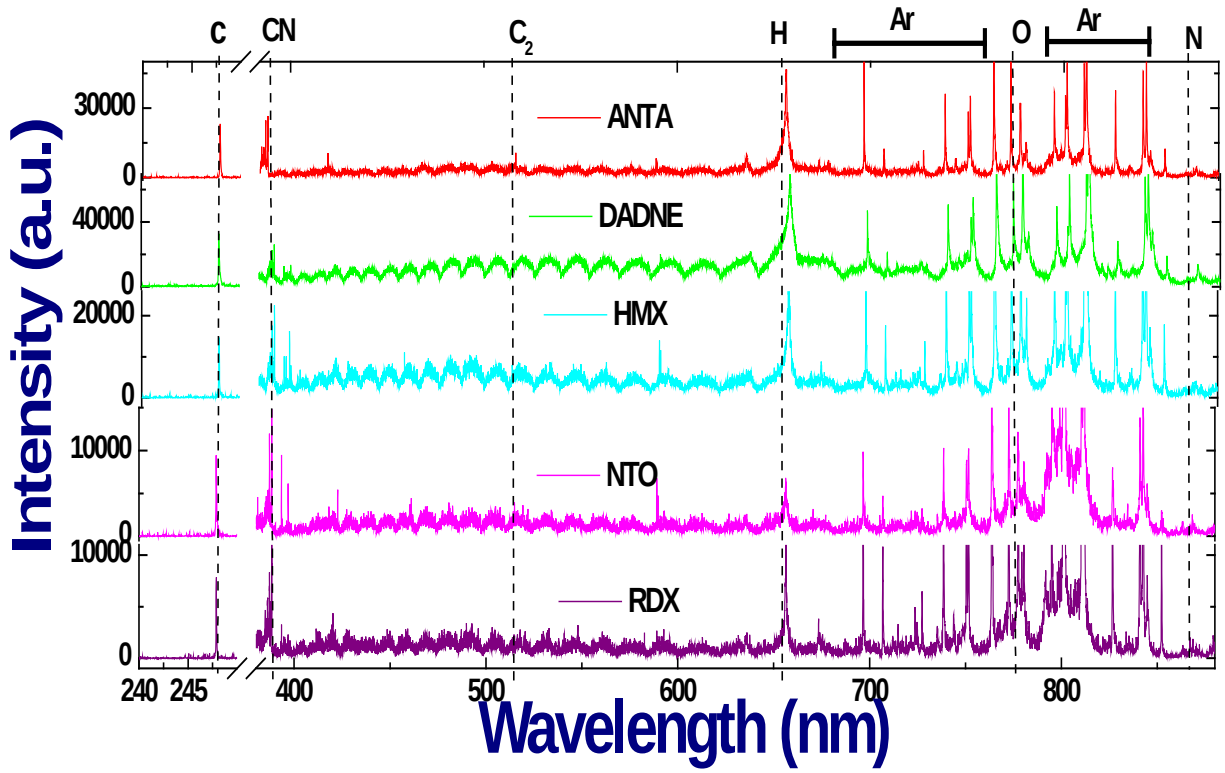

Figure 1 LIBS spectra of five explosive molecules ANTA, DADNE, HMX, NTO, and RDX obtained with fs laser excitation in argon atmospheres. A gate width of 800 ns and an initial delay of 100 ns were utilized to record the spectra. Different atomic and molecular peaks are assigned and indicated in the graphs.

To implement any statistical technique for these spectral data there is a need for a lot of pre processing procedures such as base line correction, smoothing, and normalization to be applied for the data. In the present technique there is no need of any preprocessing. Simply the 2D plot for any two elemental/molecular ratios gives reasonable classification among these samples. Moros et al. demonstrated that by plotting the intensity of two peaks in two axes they were able to distinguish explosive from non-explosives. In the present study using 2D ratio method we try to distinguish five different explosive molecules based on LIBS data. C-247.82 nm, CN-388.2 nm, H-656.2 nm, O-777.2nm and N- 868.6 nm peaks were chosen for further analysis. The areas of these peaks were calculated using Lorentzian fits. The areas were divided by transition probability and statistical weight of particular transition. Total 10 molecular/elemental ratios were computed using these areas. The 10 ratios of CN/C, CN/H, CN/O, CN/N, C/H, C/O, C/N, H/O, H/N and O/N were calculated. The 2D plot can be drawn between any of these two ratios. There can be possibly be 45 2D ratios combinations. Out of all 45 2D ratios good quality discrimination was obtained with some 2D ratios. In figure 2 we have shown such 2D ratios plots 2(a) 2D plot between CN/H Vs H/O ratios, 2(b) between CN/H and C/O, 2(c) between CN/C and H/O and 2(d) between C/H Vs C/O. A total of 190 spectra were recorded. IN figure 2 the points (corresponding to each sample spectrum) were scattered into groups and can be visualized in the forms of clusters. These plots were windows to endow the classification of these samples.

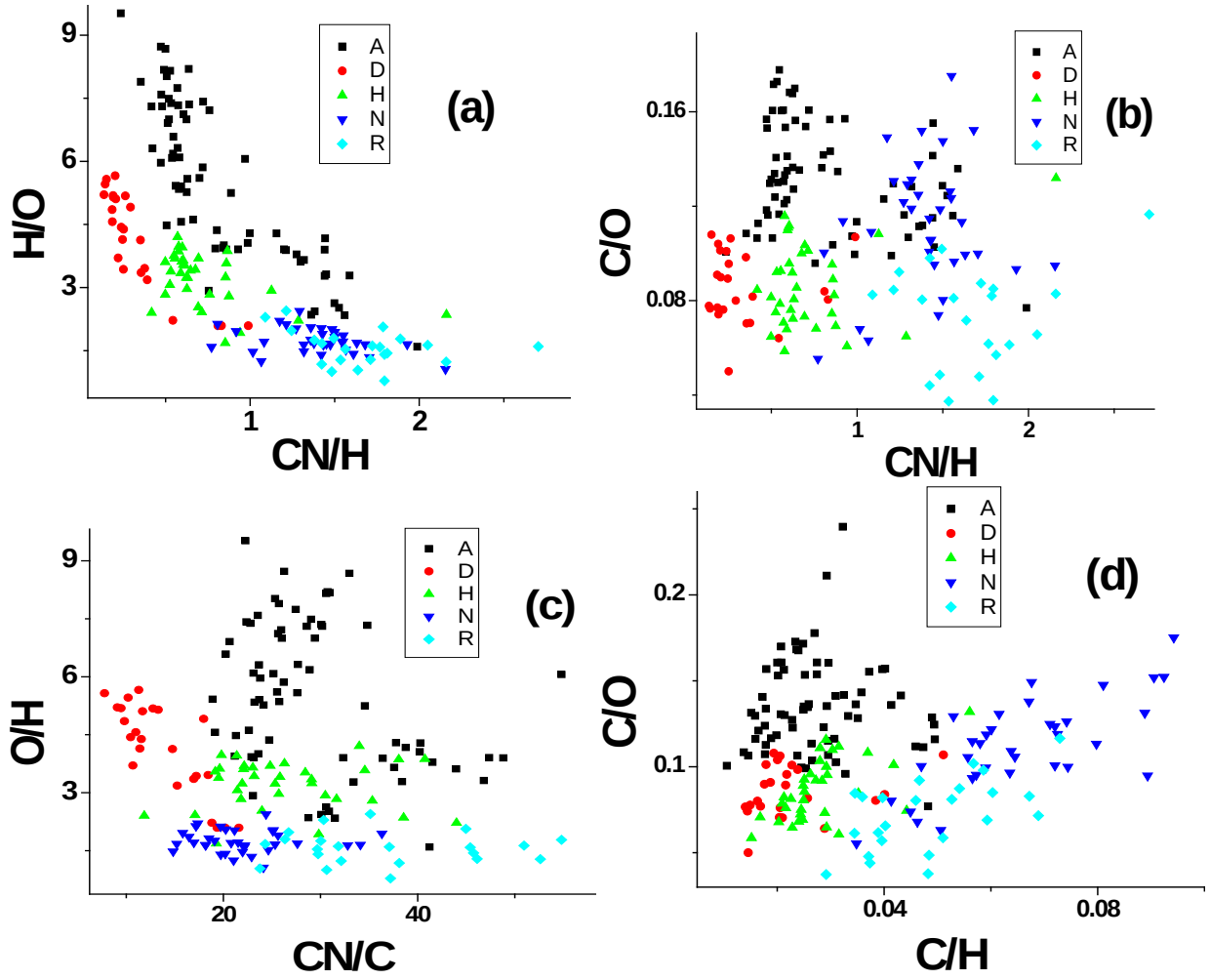

Figure 2 corresponds to plots of 2D ratios models 2(a) CN/H Vs H/O, (b) CN/H Vs C/O, (c) CN/C Vs O/H and (d) C/H Vs C/O. In the plots the points in block squares represents sample ANTA (A), red circles represents DADNE (D), green up triangles represents HMX (H), blue lower triangles corresponds to NTO (N) and violet diamonds corresponds to RDX (R) samples.

Validation using *k*- nearest-neighborhood (KNN) technique

The above 2D models provide only visualization of the data. Any classification model goal is to provide an optimal discrimination between several classes in terms of predictive performance. If we wish to know the performance of each 2D ratios model we have to apply the validation techniques. We used validation technique called *k*-nearest-neighbors (KNN) technique to validate our models. Here '*k*' is a number (integer) to be given which estimates distance between the '*k*' nearest points in the cluster. In the nearest-neighbor method we inspect the similarities with individual objects and assign objects to the class that is prevalent in the neighborhood. The KNN classification is performed on the software platform R.3.0.0 Version (statistical computing and graphics software). The whole data can be divided into two sets: one is training set to build the model with known class of samples while the other set of data can be called as testing set which is used to test the model performance. Using the given k values as an input it classifies the objects. Then the testing can be performed using test data set. After testing the result will be supplied as the predicted class values with probabilities. Then the cross validation is performed between the predicted class and actual class values of the test data set. Using the cross validation we can generate the confusion matrix, which contains information about actual and predicted classifications performed by the classification system. Table 1 is such type of matrix obtained using cross validation. From this table values individual confusion matrices for each sample can be constructed to calculate the individual class performance of each sample. The individual confusion matrix for sample H (HMX) is shown in the right side of the confusion matrix. This provides insight to what distinguishes different classes from each other. From this individual matrix we can compute the sensitivity (true positive rate), specificity (true negative rate), accuracy (proportion of correct guesses) and precision (positive predictive rate) for each individual samples. These parameters provide us the information of individual sample prediction performance. The overall accuracy of the model can be computed by the actual confusion matrix.

Confusion Matrix

Predicted value	Actual value A	D	H	N	R	
A	9	0	0	0	0	9
D	0	2	0	0	0	2
H	2	1	7	0	0	10
N	2	0	1	5	1	9
R	0	0	0	1	7	8
	13	3	8	6	8	38

for H

	True	False
+ve	7	3
-ve	1	27

Table 1 Confusion matrix obtained using cross validation between predicted values using KNN and actual values. Here A means ANTA, D- DADNE, H-HMX, N-NTO and R-RDX samples. The numbers gives the quantification of correct and wrong classification for a particular sample. The right side table is the individual confusion matrix for sample H derived from the confusion matrix, which contains the values of true positive, false positive, true negative and false negative predictions for HMX sample.

RATIO		A	D	H	N	R	Overall accuracy
CN/N vs H/N	Sensitivity	77%	100%	25%	100%	50%	
	Specificity	80%	100%	97%	88%	96%	
	Accuracy	79%	100%	82%	89%	82%	71%
	Precision	67%	100%	67%	60%	86%	
CN/H vs H/O	Sensitivity	85%	100%	75%	83%	50%	
	Specificity	100%	97%	97%	88%	96%	
	Accuracy	95%	97%	92%	87%	82%	82%
	Precision	100%	75%	86%	56%	86%	
CN/H vs C/O	Sensitivity	54%	100%	75%	50%	50%	
	Specificity	84%	100%	97%	75%	100%	
	Accuracy	74%	100%	92%	71%	84%	66%
	Precision	64%	100%	86%	27%	100%	
CN/C vs O/N	Sensitivity	77%	100%	50%	83%	40%	
	Specificity	96%	91%	87%	91%	96%	
	Accuracy	89%	92%	79%	89%	82%	68%
	Precision	91%	50%	50%	63%	80%	
CN/C vs CN/N	Sensitivity	77%	100%	25%	33%	54%	
	Specificity	76%	94%	93%	94%	92%	
	Accuracy	76%	95%	79%	84%	79%	63%
	Precision	63%	60%	50%	50%	78%	
CN/C vs H/O	Sensitivity	62%	100%	38%	100%	33%	
	Specificity	88%	97%	93%	84%	86%	
	Accuracy	79%	97%	82%	87%	74%	61%
	Precision	73%	75%	60%	55%	43%	
C/H vs C/O	Sensitivity	69%	67%	88%	83%	54%	
	Specificity	100%	100%	90%	88%	96%	
	Accuracy	89%	97%	89%	87%	82%	79%
	Precision	100%	100%	70%	56%	88%	
C/O vs H/O	Sensitivity	54%	33%	75%	67%	50%	
	Specificity	92%	97%	80%	91%	92%	
	Accuracy	79%	92%	79%	87%	79%	63%
	Precision	78%	50%	50%	57%	75%	

Table2 Performance result of different 2D ratios models. The measurement of sensitivity, specificity, accuracy and precision parameters for each and individual samples were shown in the table.

The KNN validation technique was applied for all the 45 models of 2D ratios. Some of the best performed 2D models with KNN are shown in the table 2. The model performance parameters for each sample prediction derived from individual confusion matrix of the sample for different 2D models are tabulated. The best overall accuracy (82 %) was obtained with CN/H Vs H/O ratios model. The CN/N Vs H/N, C/H Vs C/O ratios models achieved >70% overall accuracy. Remaining all models were found to be >60% accurate, which is reasonably good. The best classified among all the samples in all 2D ratios was the sample DADNE. The sample HMX was moderately classified in some models. However, since these 2D models having good predictive probability it can provide an insight in distinguishing different classes from each other.

In the KNN technique the performance depends on k value. The value of k will be crucial in classification of objects. However, there is no particular method to define a best k value. The smallest value of k gives the optimal predictions; larger values may also lead to equally good predictions. To get desired k value for good performance several cross validations with test sets were performed with different k values. The curve shown in figure 3(a) was obtained from 10 fold cross validation done with several k values. This tells that at k = 9 this model performs well. The KNN picks the neighbors in random process so there could be some deviation in finding the good k values. Hence, the best performance k value can be obtained by computing 1000 such cross validations. Figure 3(b) corresponds to best k values obtained with 1000 cross validations.

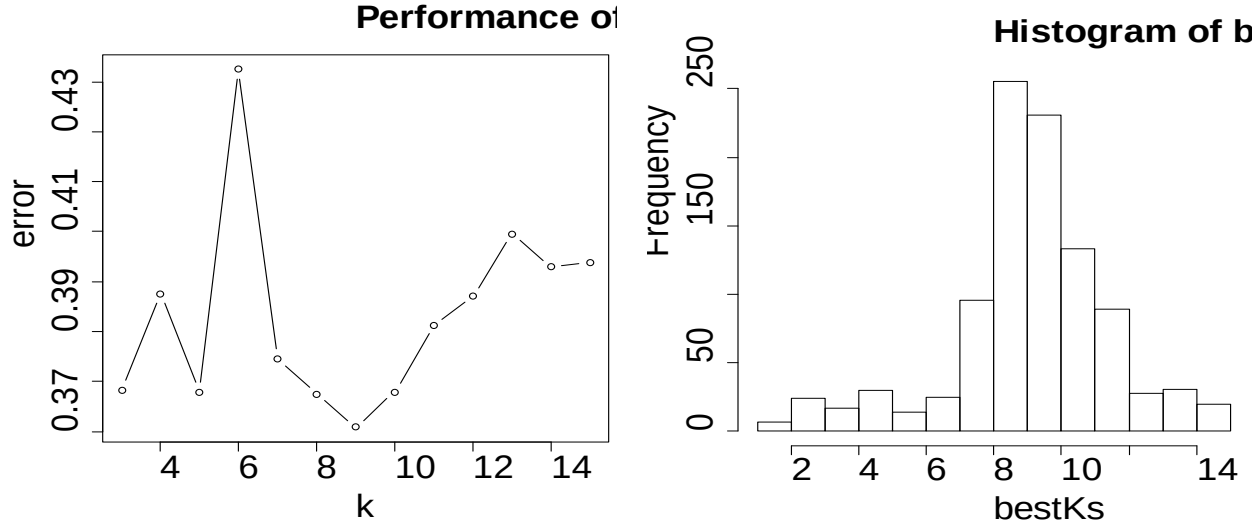

Figure 3 (a) corresponds to performance of k value obtained in 10 cross validations (b) Represents best k values performance obtained using 1000 cross validations.

This analysis suggests that using 2D ratios models we can create markers for each explosive. Further steps of this work include performing the analysis with 3D ratios models utilizing the same data. Our future goals include unambiguous detection of explosives molecules (even if mixed with PMMA matrix) with LIBS data by applying the validity of 2D and 3D ratios models.

Conclusions

The present work demonstrates that using 2D ratios combination models classification of organic explosives samples with LIBS spectral data. The classification merely achieved reasonably good predictability of each and individual organic explosive samples. The performance of all 2D ratios models was done with the KNN technique. The individual sample identification capabilities were measured using sensitivity, specificity, accuracy and precision parameters.

Acknowledgments

Financial support from DRDO, India is gratefully acknowledged. The authors also acknowledge the samples provided by HEMRL, Pune, India and P. Ravi, ACRHEM.

References

[1] J.L. Gottfried, F.C. De Lucia Jr., C.A. Munson, A.W. Miziolek, "Laser-induced breakdown spectroscopy for detection of explosives residues: A review of recent advances, challenges, and future prospects," Anal. Bioanal. Chem. 395 (2009) 283-300.

[2] F.C. De Lucia Jr., J.L. Gottfried, "Rapid analysis of energetic and geo-materials using LIBS," Mater. Today 14 (2011) 274-281.

[3] J.L. Gottfried, F.C. De Lucia Jr., C.A. Munson, A.W. Miziolek, Standoff detection of chemical and biological threats using laser-induced breakdown spectroscopy, Appl. Spectrosc. 62 (2008) 353-363.

[4] J. Moros, J.A. Lorenzo, P. Lucena, L.M. Tobaria, J.J. Laserna, "Simultaneous Raman Spectroscopy−Laser-Induced Breakdown Spectroscopy for Instant Standoff Analysis of Explosives Using a Mobile Integrated Sensor Platform," Anal. Chem. 82 (2010) 1389-1400.

[5] M. Abdelhamid, F.J. Fortes, M.A. Harith, J.J. Laserna, "Analysis of explosive residues in human fingerprints using optical catapulting–laser-induced breakdown spectroscopy," J. Anal. At. Spectrom. 26 (2011) 1445-1450.

[6] F.C. De Lucia Jr., J.L. Gottfried, C.A. Munson, A.W. Miziolek, Multivariate analysis of standoff laser-induced breakdown spectroscopy spectra for classification of explosive-containing residues, Appl. Opt. 47 (2008) G112-G122

[7] C. López-Moreno, S. Palanco, J.J. Laserna, F.C. DeLucia Jr., A.W. Miziolek, J. Rose, R.A. Walters, A.I. Whitehouse, Test of a stand-off laser-induced breakdown spectroscopy sensor for the detection of explosive residues on solid surfaces, J. Anal. Atom. Spectrom. 21 (2006) 55-60.

[8] A.W. Miziolek, V. Palleschi, and I. Schechter, eds., *Laser-Induced Breakdown Spectroscopy (LIBS): Fundamentals and Applications* (Cambridge U. Press, 2006).

[9] J.P. Singh and S.N. Thakur, eds., *Laser-Induced Breakdown Spectroscopy* (Elsevier, 2007).

[10] D.A. Rusak, B.C. Castle, B.W. Smith, J.D. Winefordner, "Fundamentals and applications of laser induced breakdown spectroscopy," Crit. Rev. Anal. Chem. 27 (1997) 257-290.

[11] D.W. Hahn and N. Omenetto, "Laser-Induced Breakdown Spectroscopy (LIBS), Part II: Review of Instrumental and Methodological Approaches to Material Analysis and Applications to Different Fields," Appl. Spectrosc. 66 (2012) 347-419.

[12] E.L. Gurevich and R. Hergenroeder, "Femtosecond laser-induced breakdown spectroscopy: Physics, applications, and perspectives," Appl. Spectrosc. 61 (2007) 233A-242A.

[13] P. Rohwetter, J. Yu, G. Mejean, K. Stelmaszczyk, E. Salmon, J. Kasparian, J.-P. Wolf, L. Woeste, "Remote LIBS with ultrashort pulses: characteristics in picosecond and femtosecond regimes," J. Anal. At. Spectrom. 19 (2004) 437-444.

[14] Y. Liu, S. Singha, T. E. Witt, Y. Cheng, R. J. Gordon, "Observation of near total polarization in the ultrafast laser ablation of Si," Appl. Phys. Lett. 93 (2008) 161502-3.

[15] J.S. Penczak, Y. Liu, and R. J. Gordon, "Polarization Resolved Laser-Induced Breakdown Spectroscopy of Al," J. Phys. Chem. A 113 (2009) 13310–13317.

[16] M. Baudelet, L. Guyon, J. Yu, J.-P. Wolf, T. Amodeo, W. Frejafon, P. Laloi, Femtosecond time-resolved laser-induced breakdown spectroscopy for detection and identification of bacteria: A comparison to the nanosecond regime, J. Appl. Phys. 99 (2006) 84701-9.

[17] M. Baudelet, L. Guyon, J. Yu, J.-P. Wolf, T. Amodeo, E. Frejafon, P. Laloi, Spectral signature of native CN bonds for bacterium detection and identification using femtosecond laser-induced breakdown spectroscopy, Appl. Phys. Lett. 88 (2006) 063901.

[18] Y. Dikmelik, C. McEnnis, J.B. Spicer, "Femtosecond laser-induced breakdown spectroscopy of explosives," Proc. SPIE 6217II (2006) 62172A.

[19] Y. Dikmelik, C. McEnnis, J.B. Spicer, "Femtosecond and nanosecond laser-induced breakdown spectroscopy of trinitrotoluene," Opt. Express 16 (2008) 5332-5337.

[20] F.C. De Lucia Jr., J.L. Gottfried, A.W. Miziolek, "Femtosecond laser-induced breakdown spectroscopy of explosives and explosive-related compounds," Opt. Express 17 (2009) 419-425.

[21] S. Venugopal Rao, S. Sreedhar, M.A. Kumar, P. Prem Kiran, Surya P. Tewari, G. Manoj Kumar, "Laser Induced Breakdown Spectroscopy of high energy materials using nanosecond, picosecond, and femtosecond pulses: Challenges and opportunities," Proc. SPIE 8173 (2011) 81731A.
[22] S. Sreedhar, G. Manoj Kumar, M. Ashwin Kumar, P. Prem Kiran, Surya P. Tewari, S. Venugopal Rao, Femtosecond and nanosecond laser induced breakdown spectroscopic studies of NTO, HMX, and RDX, Spectrochim. Acta Part B (2012) 79–80 (2013) 31–38.
[23] V. Lazic, A. Palucci, S. Jovicevic, M. Carpanese, "Detection of explosives in traces by laser induced breakdown spectroscopy: Differences from organic interferents and conditions for a correct classification," Spectrochim. Acta Part B 66 (2011) 644-655.
[24] F. C. De Lucia and J.L. Gottfried, "Classification of explosive residues on organic substrates using laser induced breakdown spectroscopy," Appl. Opt. 51 (2012) B83-B92.
[25] P. Lucena, A. Doña, L.M. Tobaria, J.J. Laserna, New challenges and insights in the detection and spectral identification of organic explosives by laser induced breakdown spectroscopy, Spectrochim. Acta Part B. 66 (2011) 12–20.
[26] F.C. De Lucia Jr., J.L. Gottfried, Characterization of a series of nitrogen-rich molecules using laser induced breakdown spectroscopy, Prop. Explos. Pyrotech. 35 (2010) 268-277.
[27] J. Moros, J. Serrano, C. Sanchez, J. Macıas and J. J. Laserna, "New chemometrics in laser-induced breakdown spectroscopy for recognizing explosive residues," J. Anal. At. Spectrom. 27 (2012) 2111–2122.